DOI: 10.1002/ejic.201100781

Systematic Expansion of Supercubane Cores in Manganese Oxo Clusters with Tricarboxylate Ligands

Yayoi Okui,[a] Florina Aurelia Catusanu,[a] Ryoko Kubota,[a] Bunsho Kure,[a] Takayuki Nakajima,[a] Tomoaki Tanase,*[a] Takashi Kajiwara,[a] Masahiro Mikuriya,[b] Hitoshi Miyasaka,[c] and Masahiro Yamashita[d]

Keywords: Manganese / Carboxylate ligands / Mixed-valent compounds / Cluster compounds / Supercubane cores / Magnetic properties

A novel class of high-nuclearity Mn_{17} and Mn_{19} mixed-valent complexes, $[Mn_{17}(\mu\text{-}O)_{12}(\mu\text{-}OMe)_2(\mu\text{-}kta)_6(MeOH)_4]$ (**1**), $[Mn_{17}(\mu\text{-}O)_{14}(\mu\text{-}kta)_6L_4]$ [L = bpy (**2a**), phen (**2b**), 4,7-Ph_2phen (**2c**), dmf (**3**)], and $[Mn_{19}(\mu\text{-}O)_{14}(\mu\text{-}kta)_6(bpy)_6]X_3$ [X = PF_6 (**4a**), BF_4 (**4b**)], were synthesized by utilizing Kemp's tricarboxylate ligands (H_3kta = *cis*,*cis*-1,3,5-trimethylcyclohexane-1,3,5-tricarboxylic acid). The complexes were characterized by X-ray crystallography and reveal mineralomimetic Mn_{13} supercubane units, $[Mn_{13}(\mu\text{-}O)_{14}]$, in which their oxidation states systematically altered, depending on their vertex face-capping ligands and Mn^{II} satellite fragments. Complex **2a** was converted by treatment with benzoic acid and $[Mn_2O_2(bpy)_4](BF_4)_3$ to a cage-type Mn_{14} complex, $[Mn_{14}(\mu\text{-}O)_{12}(\mu\text{-}OH)_6(\mu\text{-}Hkta)_6(bpy)_6](BF_4)_4$ (**5**), which show ferro- and antiferromagnetic interactions and slow magnetic relaxation at low temperature.

Introduction

Manganese oxo clusters have been intensively studied since the first finding of single-molecule magnetism (SMM) for the mixed-valent Mn_{12} complexes, $[Mn^{III}_8Mn^{IV}_4O_{12}(O_2CR)_{16}(H_2O)_4]$ (R = Ph, Me),[1] and many high-nuclearity complexes (up to Mn_{84}) have been reported with a variety of metal topologies, with an aim at developing nanostructured molecular magnetic devices.[1,2] Furthermore, mixed-valent manganese oxo clusters have attracted extensive attention with relevance to the Mn_4 oxygen-evolving center (OEC) in PS II and mineralomimetic materials.[3] From a synthetic view point, fine-tunable, bottom-up routes should be required to establish manganese clusters with their pursued functions; however, the highest-nuclearity Mn complexes have been prepared by serendipitous assembly with simple bridging ligands, such as carboxylates and alkoxides, under various conditions. Although polydentate ligands with alkoxo, phenoxo, amino, and/or imino groups were introduced occasionally, systematic synthetic methods with polycarboxylate ligands are quite limited thus far. Recently, Christou et al. have obtained the mixed-valent metal-centered cuboctahedral Mn_{13} complexes by utilizing 1,8-naphthalene-dicarboxylic acid (H_2ndc), $[Mn_{13}O_8(OR)_6(ndc)_6]$ (R = H, Me, Et),[4] and ferrocene-1,1′-dicarboxylic acid (H_2fdc), $[Mn_{13}O_8(OMe)_6(fdc)_6]$,[5] in which tridecanuclear so-called supercubane structures of $\{Mn^{II}_6Mn^{III}_6Mn^{IV}(\mu_5\text{-}O)_6(\mu_3\text{-}O)_2(\mu_3\text{-}OR)_6\}^{12+}$ are effectively stabilized by the biscarboxylate ligands, although they are not essential for the Mn_{13} topology.[4] The synthesis of mineralomimetic Mn_{13} supercubane cores, which have similar structure to that of rock salt with mixed-valent Mn ions (Scheme 1a), is still limited. However, these supercubane cores present a promising motif for the expansion and control of Mn mixed-valent giant structures. We have tried to establish this strategy by utilizing Kemp's triacid [*cis*,*cis*-1,3,5-trimethylcyclohexane-1,3,5-tricarboxylic acid (H_3kta)] (Scheme 1b),[6] since the three carboxylate groups of kta^{3-} are constrained in the same direction, which would be suitable for supporting planar metallic arrays in expanded structures from the supercubane motif. Here, we wish to report the synthesis of Mn_{17} and Mn_{19} complexes with kta^{3-} ligands, in which the supercuboidal Mn_{13} cores are surrounded by four and six Mn^{II} ions, respectively. The number of the satellite Mn^{II} ions as well as oxo and alkoxo μ_3-capping groups alter the oxidation state of the Mn_{13} cores in a specific fashion.

[a] Department of Chemistry, Faculty of Science, Nara Women's University, Kitauoya-nishi-machi, Nara, 630-8506, Japan
Fax: +81-742-20-3847
E-mail: tanase@cc.nara-wu.ac.jp
[b] Department of Chemistry, School of Science and Technology, Kwansei Gakuin University, 2-1 Gakuen, Sanda-shi, Hyogo 669-1337, Japan
[c] Division of Material Chemistry, Graduate School of Natural Science and Technology, Kanazawa University, Kakuma-machi, Kanazawa-shi, Ishikawa 920-1192, Japan
[d] Department of Chemistry, Graduate School of Science, Tohoku University, 6-3 Aramaki Aza Aoba, Aoba-ku, Sendai-shi, Miyagi 980-8578, Japan
Supporting information for this article is available on the WWW under http://dx.doi.org/10.1002/ejic.201100781.

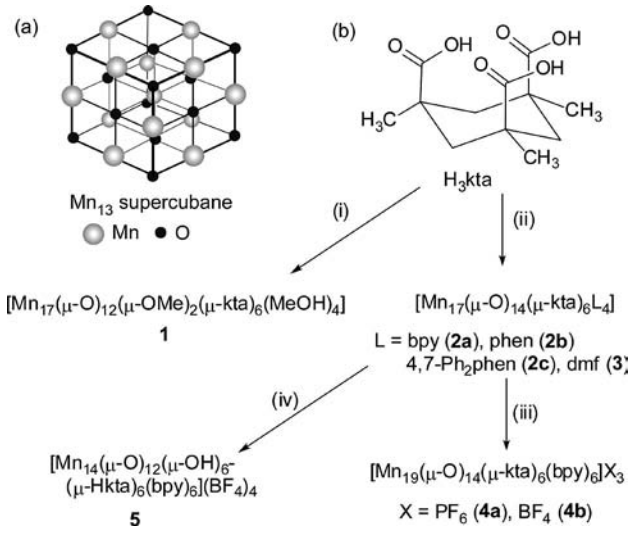

Scheme 1. The structures of Mn_{13} supercubane (a) and H_3kta with its reactions (b); (i) [nBu$_4$N][OH], $Mn(OAc)_2{\cdot}4H_2O$, MeOH; (ii) [nBu$_4$N][OH], $Mn(OAc)_2{\cdot}4H_2O$, $KMnO_4$, L (bpy, phen, 4,7-Ph_2phen, or dmf); (iii) ferrocene, $[Mn_2O_2(bpy)_4]X_3$ (X = PF_6, BF_4); (iv) PhCOOH, $[Mn_2O_2(bpy)_4](BF_4)_3$.

Results and Discussion

When $Mn(OAc)_2{\cdot}4H_2O$ was treated with H_3kta and [nBu$_4$N][OH] in an acetonitrile/acetone/methanol mixed solvent and the product was crystallized from methanol, dark brown crystals of $[Mn_{17}O_{12}(OMe)_2(kta)_6(MeOH)_4]$ (**1**) were obtained in 20% yield. The structure was determined by X-ray crystallography and reveals a supercubane core $[Mn_{13}(\mu_5\text{-O})_6(\mu_4\text{-O})_4(\mu_3\text{-O})_2(\mu_3\text{-OMe})_2]^{10+}$ surrounded by four Mn^{II}(MeOH) satellites through μ_4-oxo units; the overall Mn_{17} structure is supported by six kta^{3-} ligands and possesses a C_i symmetry (Figure 1a). The oxidation states of the Mn ions were determined by bond valence sum (BVS) analyses (Table S1)[7] and by consideration of charge, structural parameters, and Jahn–Teller distortion for the Mn^{III} centers (axial elongation for Mn4, Mn5 and planar for Mn2, Mn7). The Mn^{IV}-centered (Mn1) supercube (Figure 1b), in which the midpoints of its edges are occupied by four Mn^{II} ions (Mn3/3*, Mn6/6*) and eight Mn^{III} ions (Mn2/2*, Mn4/4*, Mn5/5*, Mn7/7*), has eight vertices bridged by two μ_3-methoxo (O7/7*), two μ_3-oxo (O1/1*), and four μ_4-oxo (O5/5*, O6/6*) groups; the latter further connect to the satellite Mn^{II} atoms (Mn8/8*, Mn9/9*), which adopt a five-coordinate trigonal-bipyramidal structure with a labile methanol coordination (τ = 0.76–0.86).[9] The six kta^{3-} ligands notably support two *trans*- and four *cis*-Mn_6O_5 planar units, which are fused to complete the Mn_{17} structure (see Figure S1); in other words, six faces of the Mn_{13} cube are supported by each kta^{3-} ligand. The structure can also be viewed as three metallic layers along the O1–Mn1–O1* [$Mn^{IV}(\mu_3\text{-O})_2$] axis; the Mn^{IV}-centered hexagonal plane (Mn1, Mn3/3*, Mn6/6*, Mn7/7*) is sandwiched by two Mn^{III} triangles [(Mn2, Mn4, Mn5*) and (Mn2*, Mn4*, Mn5)] [Figure 2a (right)]. These layers are arranged in a staggered form to make up a cuboctahedral metallic framework, which is composed of six square planes and eight equilateral triangles. The six peripheral triangles surrounding the $Mn^{IV}(\mu_3\text{-O})_2$ axis are facially capped by two MeO^- and four OMn^{II}(MeOH) fragments [Figure 2a (left)]. The oxidation state of the hexagonal Mn ions,

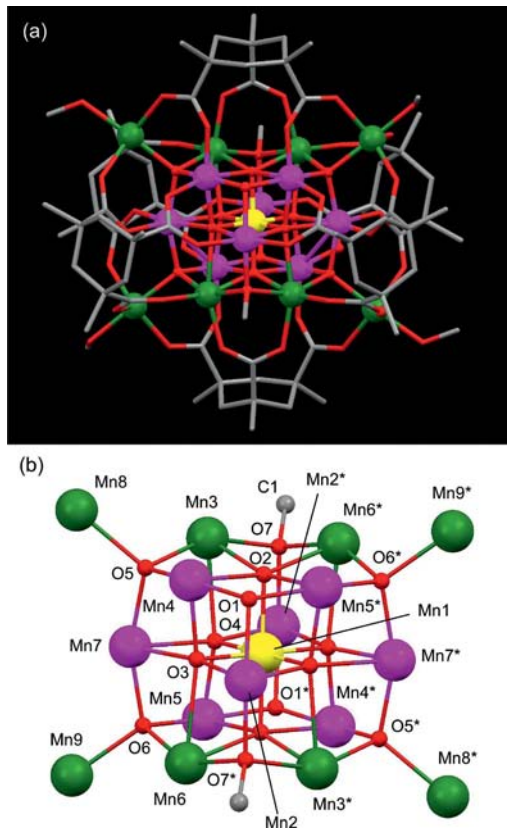

Figure 1. (a) Perspective drawing of complex **1**. The kta^{3-} ligands and MeOH are drawn as stick models and the hydrogen atoms are omitted for clarity. The Mn atoms and the atoms of the oxo and methoxy groups are drawn as arbitrary spheres. Mn^{II} (green), Mn^{III} (violet), Mn^{IV} (yellow), O (red), and C (gray). (b) Perspective view of the Mn_{17} cluster core with the atomic numbering scheme.

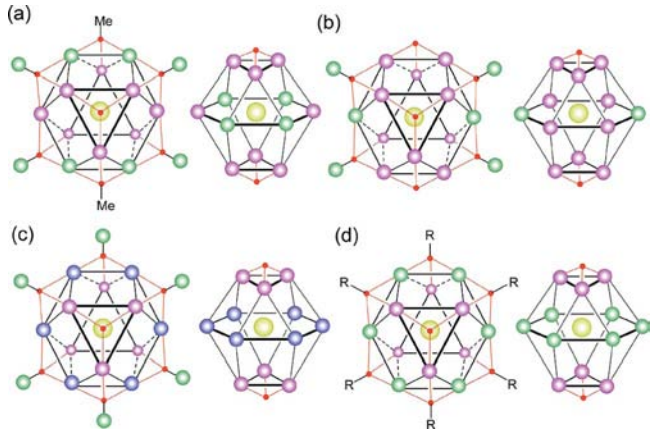

Figure 2. The three-layered metallic frameworks of (a) the Mn_{17} alkoxo complex of **1**, (b) Mn_{17} oxo complexes (**2** and **3**), (c) Mn_{19} complex **4**, and (d) Mn_{13} complexes,[4,5] viewed along (left) and vertical to (right) the $Mn^{IV}(\mu_3\text{-O})_2$ axis. R = H, Me, Et; Mn^{II} (green), Mn^{III} (violet), Mn^{IV} (yellow), $Mn^{2.5+}$ (blue), and O (red).

$\{Mn^{II}_4Mn^{III}_2\}$, is markedly different from that of the Mn_{13} supercubane complexes, $\{Mn^{II}_6\}$ (Figure 2d),[4,5] because of the introduction of four OMn^{II} satellite units instead of alk-oxo and hydroxo groups.

When an acetonitrile/acetone solution containing H_3kta and $[nBu_4N][OH]$ was added to a MeCN solution of $Mn(OAc)_2{\cdot}4H_2O$ and $KMnO_4$ in the presence of 2,2′-bipyridyl (bpy), 1,10-phenanthroline (phen), 4,7-diphenyl-1,10-phenanthroline (4,7-Ph_2phen) or *N*,*N*-dimethylformamide (dmf), a series of Mn_{17} complexes formulated as $[Mn_{17}O_{14}(kta)_6L_4]$ [L = bpy (**2a**), phen (**2b**), 4,7-Ph_2phen (**2c**), and dmf (**3**)] were synthesized in 10–35% yield (Scheme 1). The structures of **2c** and **3** were determined by X-ray crystallography and reveal a supercubane core, $[Mn_{13}(\mu_3\text{-}O)_4(\mu_4\text{-}O)_4(\mu_5\text{-}O)_6]^{10+}$, surrounded by four Mn^{II} satellite units with a 4,7-Ph_2phen and dmf ligand, which are further supported by six kta^{3-} ligands as in **1** (Figures 3 and S2). The satellite Mn^{II} ions adopt distorted $[N_2O_4]$ octahedral and $[O_5]$ trigonal-bipyramidal structures in **2c** and **3**, respectively. The overall Mn_{17} structures of **2c** and **3** apparently resemble that of **1** in that they are composed of three metallic layers [Figure 2b (right)], but the oxidation states of the hexagonal Mn ions remarkably vary from $\{Mn^{II}_4Mn^{III}_2\}$ of **1** to $\{Mn^{II}_2Mn^{III}_4\}$ upon replacement of the two μ_3-methoxy groups by two μ_3-oxo ones [Figure 2b (left)]; the oxidation states of the two triangle Mn_3 and the central Mn ions remain as $\{Mn^{III}_3\}$ and Mn^{IV}, respectively. Metal–metal interactions were investigated on the basis of the temperature dependence of the dc magnetic susceptibility measured for **1**, **2c**, and **3** (Figure S3), which indicates dominant antiferromagnetic interactions within the molecules.

Some attempts have also been made to examine the reactivity of the Mn_{17} complexes as a high-nuclearity building block or precursor. When complex **2a** was treated with ferrocene followed by $[Mn_2O_2(bpy)_4]X_3$ (X = PF_6, BF_4),[9] dark brown crystals of $[Mn_{19}O_{14}(kta)_6(bpy)_6]X_3$ [X = PF_6 (**4a**), BF_4 (**4b**)] were obtained in 24–37% yield (Scheme 1). The Mn_{19} complex cation of **4a** possesses a +3 charge and has a crystallographically imposed inversion center at the central Mn^{IV} atom (Mn1) or a *pseudo*-S_6 symmetry around the O2–Mn1–O2* $[Mn^{IV}(\mu_3\text{-}O)_2]$ axis (Figure 4). The supercubane core $[Mn_{13}(\mu_3\text{-}O)_2(\mu_4\text{-}O)_6(\mu_5\text{-}O)_6]^{9+}$ is surrounded by six Mn^{II}(bpy) satellites through the μ_4-oxo bridges that cap the peripheral Mn_3 triangles around the S_6 axis. The six kta^{3-} ligands show an essentially identical bridging mode supporting only a *cis*-Mn_6O_5 planar array (see Figure S1b).

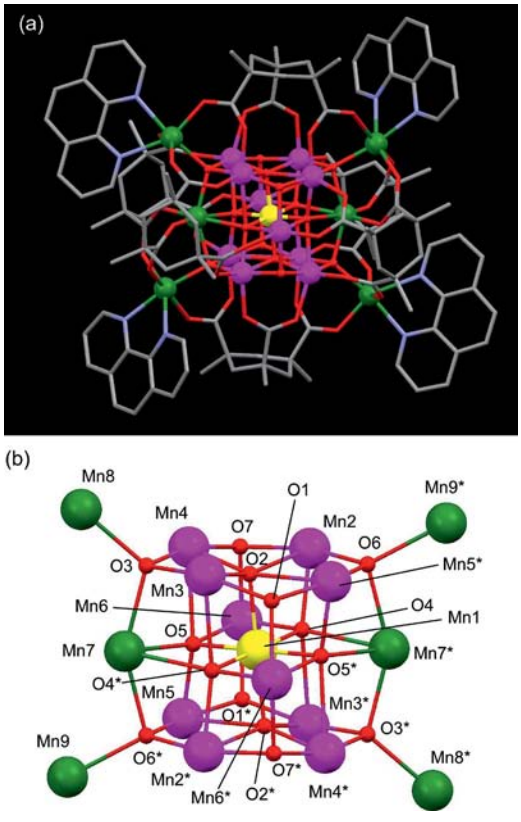

Figure 3. (a) Perspective drawing of complex **2c**. The kta^{3-} ligands and phen units are drawn as stick models, and the phenyl groups and hydrogen atoms are omitted for clarity. The Mn atoms and the atoms of the oxo groups are drawn as arbitrary spheres. Mn^{II} (green), Mn^{III} (violet), Mn^{IV} (yellow), O (red), N (light blue), and C (gray). (b) Perspective view of the Mn_{17} cluster core with the atomic numbering scheme.

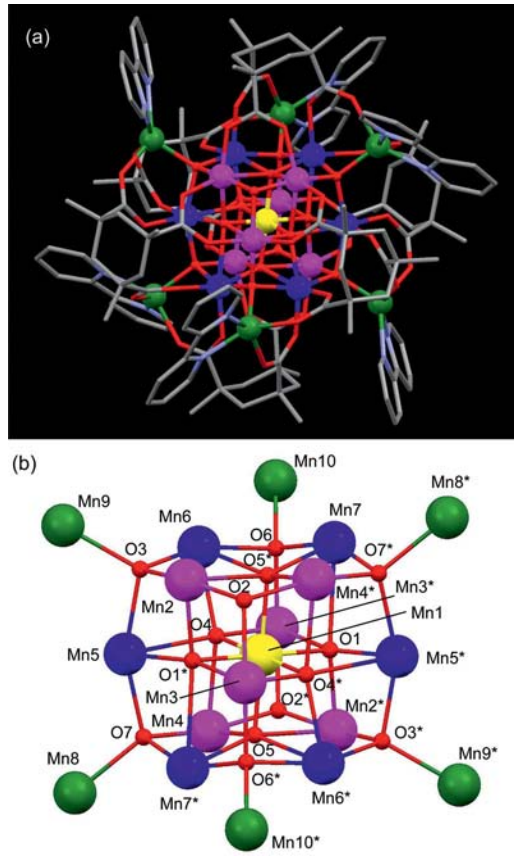

Figure 4. (a) Perspective drawing for complex cation of **4a**. The kta^{3-} ligands and bpy units are drawn as stick models and the hydrogen atoms are omitted for clarity. The Mn atoms and the atoms of the oxo groups are drawn as arbitrary spheres. Mn^{II} (green), Mn^{III} (violet), Mn^{IV} (yellow), $Mn^{2.5+}$ (blue), O (red), N (light blue), and C (gray). (b) Perspective view of the Mn_{19} cluster core with the atomic numbering scheme.

The Mn^{II} satellite ions have a distorted square-pyramidal geometry (τ = 0.11–0.19) with an $[N_2O_3]$ donor set. The most conspicuous part is observed in the middle hexagonal Mn_7 layer (Figure 2c). The Mn ions at the hexagonal vertices (Mn5/5*, Mn6/6*, Mn7/7*) exhibit an identically distorted structure between those of the Mn^{II} and Mn^{III} ions with a BVS value of 2.27–2.48 and no axial distortion, which demonstrates a delocalized oxidation state of +2.5. Given that Mn1/1*, Mn2-4/2*-4*, and Mn8-10/8*-10* ions are assigned to Mn^{IV}, Mn^{III}, and Mn^{II}, respectively, on the basis of BVS analysis, charge–valance consideration indicates that the six hexagonal Mn ions around the central Mn^{IV} ion in the middle layer should have a $\{Mn^{II}_3Mn^{III}_3\}$ oxidation state; presumably an alternative mixed-valent structure $\{Mn^{II}Mn^{III}\}_3$ might be detrapped as $\{Mn^{2.5+}\}_6$ even at the low temperature of –120 °C. Valence-detrapped Mn clusters are relatively limited,[10] and the present structure may provide a useful model to study spin-delocalized, high-nuclearity systems. Variable-temperature dc magnetic susceptibility data of **4b**, similar to those of **1**, indicate dominant antiferromagnetic interactions within the molecule (see Figure S4).

Treatment of complex **2a** in dmf with benzoic acid followed by $[Mn_2O_2(bpy)_4](BF_4)_3$ afforded a novel cage-type Mn_{14} complex, $[Mn_{14}O_{12}(OH)_6(Hkta)_6(bpy)_6](BF_4)_4$ (**5**), in 15% yield (Scheme 1). The Mn_{14} cage, $[Mn_{14}(\mu_3\text{-}O)_{12}(\mu_2\text{-}OH)_6]^{16+}$, has C_i symmetry (a *pseudo*-S_6 symmetry is expected from the crystal structure, see Figure 5)[7] and is composed of a planar $Mn^{IV}_6(\mu_3\text{-}O)_{12}$ hexagon (Mn2/2*, Mn3/3*, Mn4/4*), which is sandwiched by two $\{Mn^{III}(bpy)\}_3$ triangles (Mn5, 6*, 7*; Mn5*, 6, 7) through three μ_3-oxo groups for each layer. These features are reminiscent of the Mn_{13} supercube layered structure and are recognized to arise as a result of it opening out with removal of the central Mn^{IV} ion. Two Mn^{II} ions (Mn1/1*) are further incorporated in between each layers through three μ_3-oxo groups to the Mn^{IV}_6 layer and through three μ_2-hydroxo groups to the Mn^{III}_3 layer, to complete the Mn_{14} cage, which is supported by six $Hkta^{2-}$ ligands. The uncoordinated carboxylic group of each $Hkta^{2-}$ forms hydrogen-bonding interactions with the μ_2-hydroxo group (O···O 2.943–2.994 Å). While a similar tetradecanuclear cage structure was observed in $[Fe^{III}_{14}(bta)_6O_6(OMe)_{18}Cl_6]$ (Hbta = benzotriazole),[11] the Mn_{14} cage structure of **5** has not been reported thus far and is featured by the unprecedented $Mn^{IV}_6(\mu\text{-}O)_{12}$ hexagonal ring, which is interestingly in contrast to the Mn-centered Mn_7 hexagonal common motifs.[2a,12]

The $\chi_M T$ value of **5** (Figure S5a) decreases gradually from 32 $cm^3\,K\,mol^{-1}$ (300 K) to 26 $cm^3\,K\,mol^{-1}$ (130 K) and then rapidly increases to reach 47 $cm^3\,K\,mol^{-1}$ at 5 K; at 2 K, it falls to 40 $cm^3\,K\,mol^{-1}$. This indicates that both ferro- and antiferromagnetic interactions exist in the molecules. The preliminary ac susceptibility data were measured (Figure S5), and frequency-dependent out-of-phase (χ_M'') ac susceptibility signals are observed below ca. 2.7 K (Figure S5b), which indicate slow magnetic relaxation, although no peaks are observed.

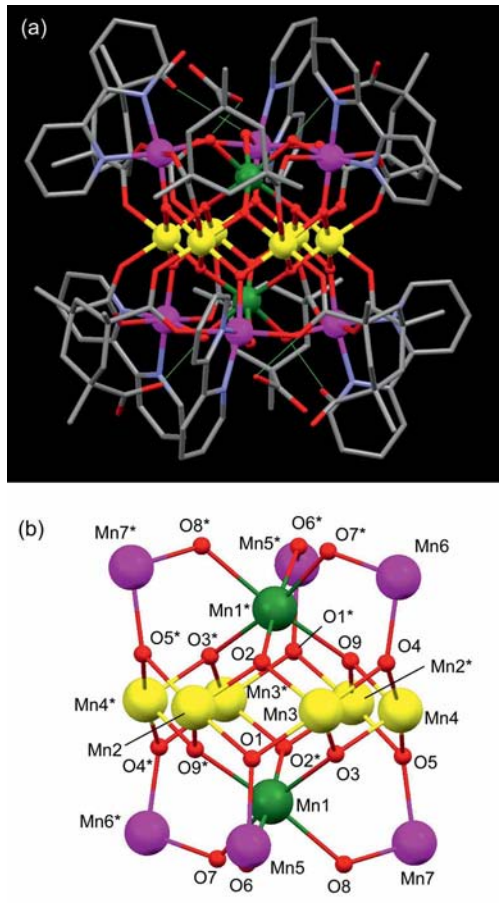

Figure 5. (a) Perspective drawing for complex cation of **5**. The $Hkta^{2-}$ ligands and bpy units are drawn as stick models and the hydrogen atoms are omitted for clarity. The Mn atoms and the atoms of the oxo and hydroxo groups are drawn as arbitrary spheres. Mn^{II} (green), Mn^{III} (violet), Mn^{IV} (yellow), O (red), N (light blue), and C (gray). The green thin lines show hydrogen bonds between COOH of $Hkta^{2-}$ and the μ_2-OH units. (b) Perspective view of the Mn_{14} cluster core with the atomic numbering scheme.

Conclusions

A novel class of high-nuclearity Mn_{17} and Mn_{19} complexes including Mn_{13} supercubane cores are synthesized by utilizing Kemp's tricarboxylate ligands, which are able to support planar Mn_6O_5 motifs. The oxidation states of the Mn_{13} supercube are systematically altered depending on its vertex face-capping ligands, which include μ-oxo, hydroxo, and alkoxo groups and μ-OMn^{II} satellite fragments, from $\{Mn^{IV}Mn^{III}_6Mn^{II}_6\}$ to $\{Mn^{IV}Mn^{III}_8Mn^{II}_4\}$, $\{Mn^{IV}Mn^{III}_6Mn^{2.5+}_6\}$, and $\{Mn^{IV}Mn^{III}_{10}Mn^{II}_2\}$. The Mn_{17} complex could also be converted to an opened-out Mn_{14} cage structure, which has a high-valent $Mn^{IV}_6(\mu\text{-}O)_{12}$ hexagonal moiety. The present results could provide a new synthetic strategy for high-nuclearity manganese oxo clusters by use of mineralomimetic $Mn_{13}O_{14}$ supercubane motifs.

Experimental Section

$[Mn_{17}O_{12}(OMe)_2(kta)_6(MeOH)_4]$·MeOH (1·MeOH): To a solution of Kemp's triacid (308 mg, 1.2 mmol) in methanol (40 mL) was added a 10% methanolic solution of tetra-*n*-butyl ammonium hydroxide [nBu$_4$N][OH] (11.5 mL, 3.6 mmol), and the solution was stirred at room temperature for 40 min. The solution was concentrated to dryness and the residue was extracted with acetone (20 mL) and acetonitrile (40 mL) with sonication. The extract was then added to a solution of $Mn(CH_3COO)_2·4H_2O$ (353 mg, 1.44 mmol) in acetonitrile (40 mL), and the mixture was stirred for 12 h. The resultant brown solution was concentrated to dryness, and the residue was extracted with methanol, which was passed through a glass filter and allowed to stand at room temperature to yield dark brown crystals of $[Mn_{17}O_{12}(OMe)_2(kta)_6(MeOH)_4]$·MeOH (**1**·MeOH).The crystals were collected, washed with methanol and diethyl ether, and dried under vacuum (106 mg, yield 20% vs. H_3kta). $C_{79}H_{116}Mn_{17}O_{55}$ (2879.70): calcd. C 32.95, H 4.06; found C 32.52, H 4.26. IR (KBr): $\tilde{\nu}$ = 1576 (s), 1469 (m), 1442 (w), 1401 (s), 1362 (w), 1209 (m), 1007 (m), 780 (m), 577 (b) cm^{-1}.

$[Mn_{17}O_{14}(kta)_6(bpy)_4]·6CH_2Cl_2·4H_2O$ (2a·6CH_2Cl_2·4H_2O): A 10% methanol solution of [nBu$_4$N][OH] (1.54 mL, 0.480 mmol) was added to a solution of Kemp's triacid (62 mg, 0.240 mmol) in methanol (10 mL) with stirring. After 30 min, the solvent was removed under reduced pressure, and the residue was dissolved in acetonitrile/acetone (2:1) solution (9 mL). The solution was then added to an acetonitrile solution (10 mL) containing $Mn(CH_3COO)_2·4H_2O$ (56 mg, 0.23 mmol), $KMnO_4$ (16 mg, 0.10 mmol), and bpy (2,2′-bipyridine) (9.7 mg, 0.062 mmol). The reaction mixture was stirred overnight and then concentrated under reduced pressure to dryness. The residue was extracted with CH_2Cl_2 (9 mL), followed by filtration to remove the inorganic salts. The extract was allowed to stand at room temperature for few days to afford dark brown crystals of $[Mn_{17}O_{14}(kta)_6(bpy)_4]·6CH_2Cl_2·4H_2O$ (**2a**·6CH_2Cl_2·4H_2O) (38 mg, yield 24% vs. H_3kta). $C_{118}H_{142}Cl_{12}Mn_{17}N_8O_{54}$ (3895.82): calcd. C 36.38, H 3.67, N 2.88; found C 36.47, H 3.72, N 2.78. IR (KBr): $\tilde{\nu}$ = 1591 (s), 1465 (m), 1440, 1392 (s), 1360, 1210 (m), 766 (m), 581 (s) cm^{-1}.

$[Mn_{19}O_{14}(kta)_6(bpy)_4](PF_6)_3$ (4a): To a dmf solution (10 mL) containing **2a**·6CH_2Cl_2·4H_2O (15 mg, 4.0 μmol) was added ferrocene (16 mg, 0.087 mmol), and the reaction solution was stirred at room temperature for 12 h. After addition of $[Mn_2O_2(bpy)_4](PF_6)_3·2H_2O$ (52 mg, 0.043 mmol), the mixture was stirred for another 12 h. The solvent was then removed under reduced pressure, and the residue was extracted with CH_2Cl_2 (ca. 9 mL), which was passed through a glass filter and allowed to stand at room temperature for 2–3 d to yield dark brown crystals of $[Mn_{19}O_{14}(kta)_6(bpy)_4](PF_6)_3·0.5$dmf (**4a**·0.5dmf) (6.1 mg, yield 37% vs. **2a**). $C_{132}H_{138}F_{18}Mn_{19}N_{12}O_{50}P_3$ (4171.30): calcd. C 38.01, H 3.33, N 4.03; found C 38.43, H 3.48, N 3.98. IR (KBr): $\tilde{\nu}$ = 1586 (s), 1466 (m), 1441 (m), 1393 (s), 1362, 1313, 1210, 1018, 847 (s), 769, 739, 557 (m) cm^{-1}.

$[Mn_{14}O_{12}(OH)_6(Hkta)_6(bpy)_6](BF_4)_4·CH_2Cl_2$ (5·CH_2Cl_2): To a dmf solution (10 mL) containing **2a**·6CH_2Cl_2·4H_2O (30 mg, 7.8 μmol) was added benzoic acid (42 mg, 0.34 mmol) with stirring. After the reaction solution was stirred at room temperature for 12 h, $[Mn_2O_2(bpy)_4](BF_4)_3·2H_2O$ (90 mg, 0.085 mmol) was added to the solution, which was stirred for another 12 h. The solvent was removed under reduced pressure, and the residue was extracted with CH_2Cl_2 (ca. 9 mL), which was passed through a glass filter and allowed to stand at room temperature for several days to give $[Mn_{14}O_{12}(OH)_6(Hkta)_6(bpy)_6](BF_4)_4·CH_2Cl_2$ (**5**·CH_2Cl_2) (4.6 mg, yield 15% vs. **2a**). $C_{133}H_{152}B_4Cl_2F_{16}Mn_{14}N_{12}O_{54}$ (3969.96): calcd. C 40.24, H 3.86, N 4.23; found C 40.28, H 3.91, N 4.25. IR (KBr): $\tilde{\nu}$ = 1603 (s), 1500, 1472, 1450 (s), 1395 (s), 1341, 1281, 1205, 1036 (s), 773 (m), 729, 664, 519 (m) cm^{-1}.

Crystallography: Crystal data for **1**·10MeOH ($C_{88}H_{152}Mn_{17}O_{64}$): M_r = 3168.08 (0.45× 0.20× 0.10 mm); triclinic; $P\bar{1}$ (no. 2); a = 14.577(2), b = 14.568(2), c = 18.376(3) Å; α = 114.264(8), β = 65.908(8), γ = 116.156(8)°; V = 3067.9(8) Å^3; Z = 1; $\rho_{calcd.}$ = 1.715 g cm^{-3}; F(000) = 1617; Mo-K_α radiation (λ = 0.71070 Å, μ = 17.77 cm^{-1}); T = –120 °C; a total of 13959 unique reflections (R_{int} = 0.036) were collected with a Rigaku/MSC Mercury CCD diffractometer ($6< 2\theta< 55.0°$); $R1$ = 0.053 [10309 reflections, $I>2\sigma(I)$]; $wR2$ = 0.136 for 783 variables. Crystal data for **2c**·8CH_2Cl_2·8H_2O ($C_{176}H_{186}Cl_{16}Mn_{17}N_8O_{58}$): M_r = 4842.62 (0.20× 0.20× 0.05 mm); triclinic; $P\bar{1}$ (no. 2); a = 17.850(3), b = 17.751(2), c = 17.664(2) Å; α = 97.431(4), β = 110.184(5), γ = 97.497(3)°; V = 5116.2(12) Å^3; Z = 1; $\rho_{calcd.}$ = 1.572 g cm^{-3}; F(000) = 2459; Mo-K_α radiation (λ = 0.71070 Å, μ = 12.97 cm^{-1}); T = –120 °C; a total of 22956 unique reflections (R_{int} = 0.061) were collected with a Rigaku/MSC Mercury CCD diffractometer ($6< 2\theta< 55.0°$); $R1$ = 0.107 [18193 reflections, $I>2\sigma(I)$]; $wR2$ = 0.302 for 1253 variables. Crystal data for **3**·10CH_2Cl_2 ($C_{94}H_{138}Cl_{20}Mn_{17}N_4O_{54}$): M_r = 3831.12 (0.50× 0.45× 0.43 mm); monoclinic; $P2_1/n$ (no. 14); a = 19.6220(9), b = 18.9211(9), c = 18.6083(8) Å; β = 91.503(4)°; V = 6906.3(5) Å^3; Z = 2; $\rho_{calcd.}$ = 1.842 g cm^{-3}; F(000) = 3854; Mo-K_α radiation (λ = 0.71070 Å, μ = 19.65 cm^{-1}); T = –120 °C; a total of 15536 unique reflections (R_{int} = 0.019) were collected with a Rigaku/MSC Mercury CCD diffractometer ($6< 2\theta< 55.0°$); $R1$ = 0.040 [14051 reflections, $I>2\sigma(I)$]; $wR2$ = 0.104 for 857 variables. Crystal data for **4a**·11CH_2Cl_2 ($C_{143}H_{160}Cl_{22}F_{18}Mn_{19}N_{12}O_{50}$): M_r = 5105.57 (0.35× 0.30× 0.30 mm); triclinic; $P\bar{1}$ (no. 2); a = 16.7822(4), b = 19.5146(4), c = 19.7290(5) Å; α = 60.257(7), β = 70.382(9), γ = 87.386(11)°; V = 5226.2(2) Å^3; Z = 1; $\rho_{calcd.}$ = 1.622 g cm^{-3}; F(000) = 2558; Mo-K_α radiation (λ = 0.71070 Å, μ = 14.93 cm^{-1}); T = –120 °C; a total of 23114 unique reflections (R_{int} = 0.035) were collected with a Rigaku/MSC Mercury CCD diffractometer ($6< 2\theta< 55.0°$); $R1$ = 0.119 [22138 reflections, $I>2\sigma(I)$]; $wR2$ = 0.334 for 1304 variables. Crystal data for **5**·4CH_2Cl_2·23H_2O ($C_{136}H_{204}B_4Cl_8F_{16}Mn_{14}N_{12}O_{77}$): M_r = 4639.11 (0.20× 0.20× 0.15 mm); triclinic; $P\bar{1}$ (no. 2); a = 17.4934(2), b = 17.9290(1), c = 19.0966(7) Å; α = 76.786(19), β = 72.239(17), γ = 65.209(16)°; V = 5143.1(8) Å^3; Z = 1; $\rho_{calcd.}$ = 1.498 g cm^{-3}; F(000) = 2370; Mo-K_α radiation (λ = 0.71070 Å, μ = 10.30 cm^{-1}); T = –120 °C; a total of 23144 unique reflections (R_{int} = 0.038) were collected with a Rigaku/MSC Mercury CCD diffractometer ($6< 2\theta< 55.0°$); $R1$ = 0.112 [18028 reflections, $I>2\sigma(I)$]; $wR2$ = 0.338 for 1280 variables. CCDC-828109 (**1**), -828110 (**2c**), -828111 (**3**), -828112 (**4a**), and -828113 (**5**) contain the supplementary crystallographic data for this paper. These data can be obtained free of charge from the Cambridge Crystallographic Data Centre via www.ccdc.cam.ac.uk/data_request/cif. The perspective plots of complex **3** are available in the Supporting Information.

Supporting Information (see footnote on the first page of this article): Synthetic details (**2b**, **2c**, **3**, and **4b**), BVS analyses for **1**, **2c**, **3**, **4a**, and **5**, the bridging structures of kta^{3-}, the X-ray structure of **3**, dc magnetic data for **1**, **2c**, **3**, **4b**, and **5**, and ac magnetic data for **5** are presented.

Acknowledgments

This work was partly supported by Grants-in-Aid for Scientific Research and by the Ministry of Education, Science, Sports, and Culture of Japan for Priority Area 2107 (no. 22108521). T. T. is grateful to Nara Women's University for a research project grant.

[1] a) R. Sessoli, H.-L. Tsai, A. R. Schake, S. Wang, J. B. Vincent, K. Folting, D. Gatteschi, G. Christou, D. N. Hendrickson, *J. Am. Chem. Soc.* **1993**, *115*, 1804–1816; b) R. Sessoli, D. Gatteschi, A. Caneschi, M. A. Novak, *Nature* **1993**, *365*, 141–143; c) D. Gatteschi, R. Sessoli, *Angew. Chem.* **2003**, *115*, 278–309; *Angew. Chem. Int. Ed.* **2003**, *42*, 268–297; d) R. Winpenny (Ed.), *Single-Molecule Magnets and Related Phenomena*, Springer Heidelberg, **2010**; e) R. Winpenny (Ed.), *Molecular Cluster Magnets, World Scientific Series in Nanoscience and Nanotechnology*, World Scientific Pub. Co. New Jersey, **2011**.

[2] a) G. E. Kostakis, A. M. Ako, A. K. Powell, *Chem. Soc. Rev.* **2010**, *39*, 2238–2271; b) A. J. Tasiopoulos, A. Vinslava, W. Wernsdorfer, K. A. Abboud, G. Christou, *Angew. Chem.* **2004**, *116*, 2169–2173; *Angew. Chem. Int. Ed.* **2004**, *43*, 2117–2121; c) R. T. W. Scott, S. Parsons, M. Murugesu, W. Wernsdorfer, G. Christou, E. K. Brechin, *Angew. Chem.* **2005**, *117*, 6698–6701; *Angew. Chem. Int. Ed.* **2005**, *44*, 6540–6543; d) M. Soler, W. Wernsdorfer, K. Folting, M. Pink, G. Christou, *J. Am. Chem. Soc.* **2004**, *126*, 2156–2165; e) C. Dendrinou-Samara, M. Alexiou, C. M. Zaleski, J. W. Kampf, M. L. Kirk, D. P. Kessissoglou, V. L. Pecoraro, *Angew. Chem.* **2003**, *115*, 3893–3896; *Angew. Chem. Int. Ed.* **2003**, *42*, 3763–3766; f) M. Murugesu, M. Habrych, W. Wernsdorfer, K. A. Abboud, G. Christou, *J. Am. Chem. Soc.* **2004**, *126*, 4766–4767; g) S. Maheswaran, G. Chastanet, S. J. Teat, T. Mallah, R. Sessoli, W. Wernsdorfer, R. E. P. Winpenny, *Angew. Chem.* **2005**, *117*, 5172–5176; *Angew. Chem. Int. Ed.* **2005**, *44*, 5044–5048; h) E. E. Moushi, T. C. Stamatatos, W. Wernsdorfer, V. Nastopoulos, G. Christou, A. J. Tasiopoulos, *Inorg. Chem.* **2009**, *48*, 5049–5051.

[3] a) K. N. Ferreira, T. M. Iverson, K. Maghlaoui, J. Barber, S. Iwata, *Science* **2004**, *303*, 1831–1838; b) B. Loll, J. Kern, W. Saenger, A. Zouni, J. Biesiadka, *Nature* **2005**, *438*, 1040–1044; c) J. Yano, K. Yachandra, *Inorg. Chem.* **2008**, *47*, 1711–1726; d) V. L. Pecoraro, W.-Y. Hsieh, *Inorg. Chem.* **2008**, *47*, 1765–1778; e) M. Yagi, M. Kaneko, *Chem. Rev.* **2001**, *101*, 21–35; f) C. Tommos, G. T. Babcock, *Acc. Chem. Res.* **1998**, *31*, 18–25; g) W. Rüttinger, C. Dismukes, *Chem. Rev.* **1997**, *97*, 1–24; h) E. Bauerlein, *Angew. Chem.* **2003**, *115*, 636–664; *Angew. Chem. Int. Ed.* **2003**, *42*, 614–641; i) N. Mita, A. Maruyama, A. Usui, T. Higashihara, Y. Hariya, *Geochem. J.* **1994**, *28*, 71–80.

[4] a) C. Lampropoulos, C. Koo, S. O. Hill, K. Abboud, G. Christou, *Inorg. Chem.* **2008**, *47*, 11180–11190; b) Z. Sun, P. K. Gantzel, D. N. Hendrickson, *Inorg. Chem.* **1996**, *35*, 6640–6641.

[5] a) M. Kondo, R. Shinagawa, M. Miyazawa, M. K. Kabir, Y. Irie, T. Horiba, T. Naito, K. Maeda, S. Utsuno, F. Uchida, *Dalton Trans.* **2003**, 515–516; b) A. Masello, M. Murugesu, K. A. Abboud, G. Christou, *Polyhedron* **2007**, *26*, 2276–2280.

[6] D. S. Kemp, K. S. Petrakis, *J. Org. Chem.* **1981**, *46*, 5140–5143.

[7] a) W. Liu, H. H. Thorp, *Inorg. Chem.* **1993**, *32*, 4102–4105; b) G. J. Palenik, *Inorg. Chem.* **1997**, *36*, 4888–4890.

[8] A. W. Addison, T. N. Rao, J. Reedijk, J. van Rijn, G. C. Verschoor, *J. Chem. Soc., Dalton Trans.* **1984**, 1349–1356.

[9] S. R. Cooper, M. Calvin, *J. Am. Chem. Soc.* **1977**, *99*, 6623–6630.

[10] a) J. M. Clemente-Juan, E. Coronado, A. Forment-Aliaga, A. Gaita-Arino, C. Gimenez-Saiz, F. M. Romero, W. Wernsdorfer, R. Biagi, V. Corradini, *Inorg. Chem.* **2010**, *49*, 386–396; b) M. Sorai, M. Nakano, Y. Miyazaki, *Chem. Rev.* **2006**, *106*, 976–1031; c) E. K. Brechin, W. Clegg, M. Murrie, S. Parsons, S. J. Teat, R. E. P. Winpenny, *J. Am. Chem. Soc.* **1998**, *120*, 7365–7366.

[11] D. M. Low, L. F. Jones, A. Bell, E. K. Brechin, T. Mallah, E. Rivière, S. J. Teat, E. J. L. McInnes, *Angew. Chem.* **2003**, *115*, 3911–3914; *Angew. Chem. Int. Ed.* **2003**, *42*, 3781–3784.

[12] a) A. Ferguson, K. Thomson, A. Parkin, P. Cooper, C. J. Milios, E. K. Brechin, M. Murrie, *Dalton Trans.* **2007**, 728–730; b) M. A. Bolcar, S. M. J. Aubin, K. Folting, D. N. Hendrickson, G. Christou, *Chem. Commun.* **1997**, 1485–1486; c) G. L. Abbati, A. Cornia, A. C. Farbretti, A. Caneschi, D. Gatteschi, *Inorg. Chem.* **1998**, *37*, 3759–3766.

Received: July 27, 2011
Published Online: August 24, 2011

